# Low-energy magnetic excitations from the $Fe_{1+y-z}(Ni/Cu)_zTe_{1-x}Se_x$ system

Zhijun Xu,[1,2,3] Jinsheng Wen,[2,3,4] J. Schneeloch,[1,5] A. D. Christianson,[6] R. J. Birgeneau,[2,3] Genda Gu,[1] J. M. Tranquada,[1] and Guangyong Xu[1]

[1]*Condensed Matter Physics and Materials Science Department, Brookhaven National Laboratory, Upton, New York 11973, USA*

[2]*Physics Department, University of California, Berkeley, California 94720, USA*

[3]*Materials Science Division, Lawrence Berkeley National Laboratory, Berkeley, California 94720, USA*

[4]*Center for Superconducting Physics and Materials, National Laboratory of Solid State Microstructures and Department of Physics, Nanjing University, Nanjing 210093, China*

[5]*Department of Physics, Stony Brook University, Stony Brook, New York 11794, USA*

[6]*Quantum Condensed Matter Division, Oak Ridge National Laboratory, Oak Ridge, Tennessee 37831, USA*

(Received 4 April 2014; revised manuscript received 14 May 2014; published 28 May 2014)

We report neutron scattering measurements on low-energy ($\hbar\omega \sim 5$ meV) magnetic excitations from a series of $Fe_{1+y-z}(Ni/Cu)_zTe_{1-x}Se_x$ samples which belong to the "11" Fe-chalcogenide family. Our results suggest a strong correlation between the magnetic excitations near (0.5,0.5,0) and the superconducting properties of the system. The low-energy magnetic excitations are found to gradually move away from (0.5,0.5,0) to incommensurate positions when superconductivity is suppressed, either by heating or chemical doping, confirming previous observations.

DOI: 10.1103/PhysRevB.89.174517 PACS number(s): 74.70.Xa, 75.25.−j, 75.30.Fv, 61.05.fg

## I. INTRODUCTION

The role of magnetism is one of the key issues concerning the mechanism of high temperature superconductivity [1–3]. While static magnetic order appears to compete with superconductivity, the presence of magnetic excitations is, on the other hand, highly correlated with the occurrence of electron pairing in high-$T_c$ cuprates [4–12] as well as the Fe-based superconductors [2,3,13]. Direct evidence that the magnetic spins and electron pairs interact is provided by the appearance of the "spin resonance" [14–20] at the superconducting phase transition—a sharp increase of the magnetic scattering intensity at the resonance energy $E_r$ which is related to the size of the superconducting gap. Despite the change of magnetic scattering intensities, the magnetic dispersion itself, i.e., the variation of the magnetic excitation energy with momentum, is normally not affected by superconductivity.

Recent results from the $FeTe_{1-x}Se_x$ system (the "11" system) show a surprising exception to such behavior [21,22]. Within the superconducting phase, low-energy magnetic excitations near the in-plane wave vector $\mathbf{Q}_{AF} = (0.5,0.5)$ (using the two-Fe unit cell) tend to disperse outwards along the transverse direction with increasing energy, and form a U-shaped dispersion, with the bottom of the dispersion, at $E \approx E_r$, located at $\mathbf{Q}_{AF}$. When the system is heated to temperatures well above the superconducting transition $T_c$, this dispersion changes to two columns, where the low-energy magnetic excitations move away from $\mathbf{Q}_{AF}$. The incommensurate low-energy magnetic excitations are also observed for nonsuperconducting compositions [21–24]. These results suggest an unusual connection between the locations of the low-energy magnetic excitations in reciprocal space and the superconducting properties of the materials.

In this paper, we report systematic studies of the low-energy magnetic excitations in a series of single crystal samples of the "11" system. The samples studied are listed in Table I. These include samples of $Fe_{1+y}Te_{1-x}Se_x$, which are labeled with the percentage of Se and a prefix of SC, for superconducting (with $y = 0$), or NSC, for nonsuperconducting, due to excess Fe. Samples with Ni or Cu substitution are labeled by the type and percentage of dopant (such as Ni02 for 2% Ni substitution); these include both superconducting and nonsuperconducting samples.

Our results clearly show that at low temperature, the low-energy ($\hbar\omega \sim 5$ meV) magnetic excitations in superconducting samples are commensurate with $\mathbf{Q}_{AF}$, while in nonsuperconducting samples they are split incommensurately about $\mathbf{Q}_{AF}$, as indicated schematically in Fig. 1(b). For the nonsuperconducting samples, there is very little change in the low-energy spectra for temperatures between 4 and 100 K. In contrast, the excitations in the superconducting samples inevitably cross over from commensurate to incommensurate at a temperature $T^*$ well above $T_c$. The incommensurability $\delta$ found in all samples at 100 K shows remarkably little variation with chemical composition. The spectral weight of the low-energy magnetic excitations has little temperature dependence in the normal state and also does not change much with chemical composition. The crossover temperature $T^*$ varies approximately linearly with $T_c$, further confirming its connection to superconductivity.

## II. EXPERIMENTAL DETAILS

The single-crystal samples used in this experiment were grown by a unidirectional solidification method [25] at Brookhaven National Laboratory. Their nominal compositions and superconducting properties are listed in Table I. The bulk susceptibilities, measured with a superconducting quantum interference device (SQUID) magnetometer, are shown in Fig. 1(a). Neutron scattering experiments were carried out on the triple-axis spectrometer HB-3 located at the High Flux Isotope Reactor (HFIR) at Oak Ridge National Laboratory (ORNL). We used beam collimations of 48′-80′-S-80′-120′ (S = sample) with a fixed final energy of 14.7 meV and a pyrolytic graphite filter after the sample. The inelastic scattering measurements have been performed in the $(HK0)$

 ©2014 American Physical Society

TABLE I. List of the $Fe_{1+y-z}(Ni/Cu)_zSe_xTe_{1-x}$ samples used in our measurements, with their nominal composition, superconducting transition temperature ($T_c$), crossover temperature ($T^*$), and incommensurability $\delta$ at 100 K.

| Sample | Compound | $T_c$ (K) | $T^*$ (K) | $\delta$ (r.l.u.) |
|---|---|---|---|---|
| SC30 | $FeTe_{0.7}Se_{0.3}$ | 14 | 25 | 0.184 |
| SC50 | $FeTe_{0.5}Se_{0.5}$ | 15 | 55 | 0.176 |
| SC70 | $FeTe_{0.3}Se_{0.7}$ | 14 | 50 | 0.183 |
| NSC45 | $Fe_{1.08}Te_{0.55}Se_{0.45}$ | | | 0.157 |
| Ni02 | $Ni_{0.02}Fe_{0.97}Te_{0.55}Se_{0.45}$ | 12 | 35 | 0.200 |
| Ni04 | $Ni_{0.04}Fe_{0.95}Te_{0.55}Se_{0.45}$ | 8 | 30 | 0.210 |
| Ni10 | $Ni_{0.1}Fe_{0.9}Te_{0.55}Se_{0.45}$ | | | 0.181 |
| Cu10 | $Cu_{0.1}Fe_{0.9}Te_{0.5}Se_{0.5}$ | | | 0.161 |

scattering plane, along the transverse direction through $\mathbf{Q}_{AF}$, as indicated in Fig. 1(b). The lattice constants for these sample are $a = b \approx 3.8$ Å and $c \approx 6.1$ Å, using a unit cell containing two Fe atoms. The data are described in reciprocal lattice units (r.l.u.) of $(a^*,b^*,c^*) = (2\pi/a, 2\pi/b, 2\pi/c)$. All data have been normalized into absolute units of $\mu_B^2$ eV$^{-1}$/Fe based on measurements of incoherent elastic scattering from the samples [26]. In the normalization process, the incoherent elastic scattering intensities are assumed to be coming entirely from the sample. This could slightly overestimate the resolution volume, and therefore underestimate the resulting magnetic scattering $S(\mathbf{Q},\omega)$. No static order around (0.5, 0, 0.5) was found in any of these samples, except for SC30 and NSC45 [27].

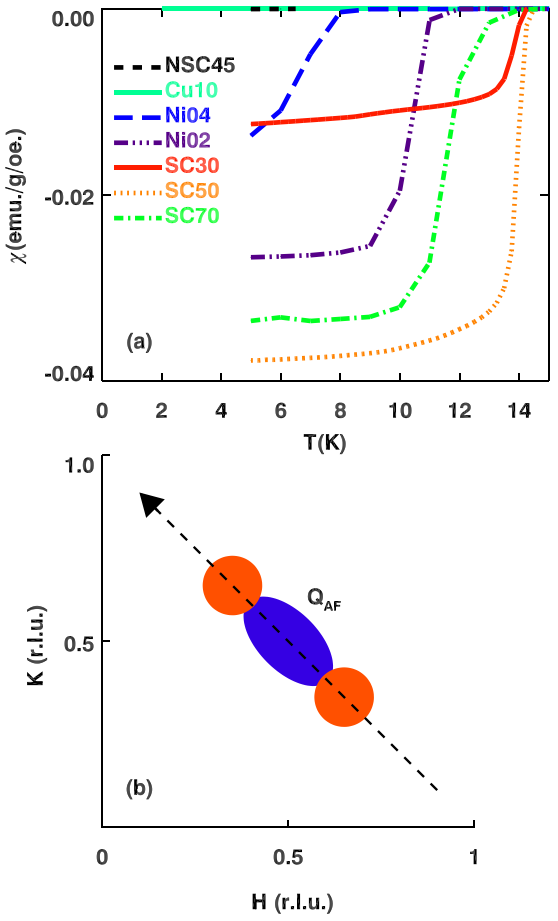



FIG. 1. (Color online) (a) ZFC magnetization measurements by SQUID with a 5 Oe field perpendicular to the *a*-*b* plane for all samples: SC30 (red solid line), SC50 (orange dotted), SC70 (green dot-dashed), Ni04 (blue long-dashed), Ni02 (purple 3-dot dashed), Cu10 (teal solid) and NSC45 (black short dashed). (b) A schematic diagram of neutron scattering measurements described in this paper. The scattering plane corresponds to (HK0), and our constant-energy scans are always performed along the transverse direction across $\mathbf{Q}_{AF} = (0.5,0.5,0)$. The (blue) ellipse and two (orange) circle regions are the locations of low-energy magnetic excitations measured in the superconducting and nonsuperconducting samples, respectively.

## III. RESULTS AND DISCUSSIONS

Unlike in the parent compound where the low-energy magnetic excitations are focused near the (0.5,0) in-plane wave vector and highly sensitive to the excess Fe in the sample [28–33], in the superconducting 11 samples, previous work [21,25] has indicated that the low-energy spin excitations are mainly distributed along the transverse direction about $\mathbf{Q}_{AF}$ and that the major changes occur around the resonance energy. Hence, we chose to focus on constant-energy scans along the path shown in Fig. 1(b). The temperature evolutions of the magnetic excitations at $\hbar\omega = 5$ meV for four samples are plotted in Fig. 2. For the bulk superconducting samples SC50

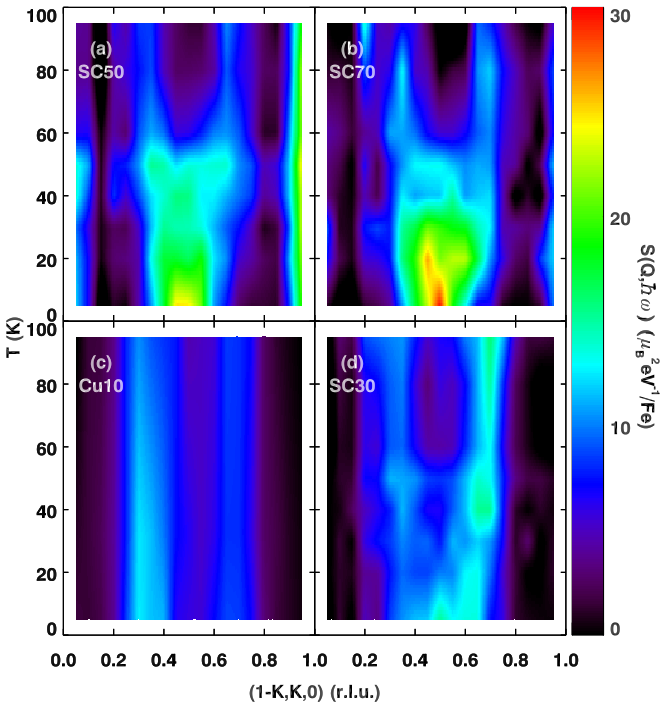



FIG. 2. (Color online) Thermal evolution of the magnetic scattering at $\hbar\omega$=5 meV. The data are measured by scans through $\mathbf{Q}_{AF}$ along the transverse direction. Contour intensity maps are plotted in temperature–wave-vector space for different samples: (a) SC50, (b) SC70, (c) Cu10 and (d) SC30. The data have been smoothed. For (a), (b), and (d), data were measured at 5, 20, 30, 40, 50, 60, 80, 100 K; for (c), measurements were at 5, 25, and 100 K. The additional intensities near the edge of the intensity map in (a) and (b) are low-energy phononlike excitations appearing near (1,0,0) and (0,1,0) positions. The nature of these intensities are still under investigation.

and SC70, shown in Figs. 2(a) and 2(b), the results are similar to those from the Ni04 sample presented in Ref. [21]. The magnetic excitation peaks clearly change from incommensurate to commensurate upon cooling. Since the change is continuous in a broad temperature range, it is hard to uniquely determine a crossover temperature. We define the crossover temperature $T^*$ as the midpoint temperature between the lowest temperature where the spectrum clearly consists of two separated peaks and the highest temperature where the spectrum clearly consists of one single peak. For nonsuperconducting sample Cu10, the results are shown in Fig. 2(c). Similar results are obtained from NSC45 and Ni10, where the incommensurate magnetic excitations show very little change for temperatures up to 100 K [21]. In the case of the SC30 sample, the results are slightly more complicated [see Fig. 2(d)]. Here, even at base temperature, the intensity profile already shows signs of extra peaks away from $\mathbf{Q}_{\mathrm{AF}}$, in addition to the central peak. $T^*$ is also relatively low despite the fact that $T_c = 14$ K is similar to the SC50 and SC70 samples. Our previous work [27] suggests that a mixture of superconducting and nonsuperconducting phases may exist in this sample; such phase separation has also been suggested by other groups [34]. The temperature evolution can be understood based on considering contributions from the coexisting superconducting and nonsuperconducting regions at low temperature; all regions become nonsuperconducting above $T_c$.

In Fig. 3, we show constant-energy scans, for select temperatures, performed at 5 and 6.5 meV. At $T = 5$ K, the data for the strongly superconducting samples show clearly commensurate single peaks; the lines through these data sets correspond to a fit by a Gaussian function. In contrast, the data for the NSC45 sample clearly shows incommensurate peaks, which were fit by a pair of symmetric Gaussian functions. The data from the SC30 sample, as discussed above, were fit by a central Gaussian function representing the contribution from the superconducting phase, plus a pair of symmetric Gaussian functions away from $\mathbf{Q}_{\mathrm{AF}}$, representing contribution from the nonsuperconducting phase. When the superconducting samples are heated to 20 K, just above $T_c$, the extra intensity due to the spin resonance disappears, but intensity profiles still remain commensurate. This situation clearly changes on warming to 100 K, where the signal is split into two symmetric incommensurate peaks. For all samples, the incommensurability of the peaks, as well as their intensities, at 100 K are remarkably similar.

The integrated intensities of the fitted peaks are plotted as a function of temperature in Fig. 4. Regardless of the sample character, the integrated intensity in the normal state shows little temperature dependence, and the major changes occur around the superconducting transition when the spin resonance appears. This insensitivity of low-energy spectra weight to temperature and composition is consistent with previous reports [35,36]. For the superconducting samples, it is interesting to note that there is little change in integrated intensity on passing through $T^*$. Whether this indicates a real conservation of low-energy spectral weight or is simply

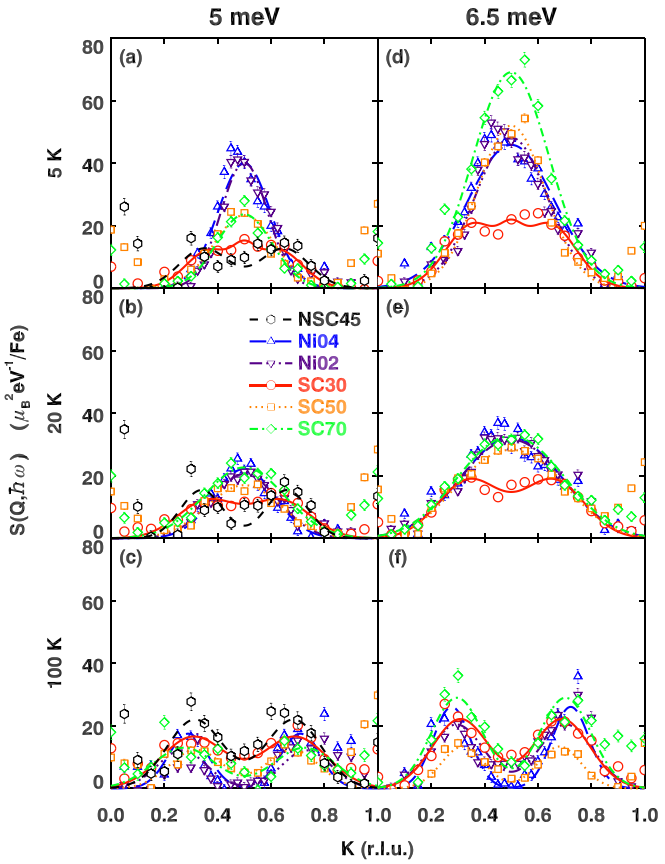



FIG. 3. (Color online) Constant energy scans through $\mathbf{Q}_{\mathrm{AF}}$ along $(1-K,K,0)$ for different samples: SC30 (red circles), SC50 (orange squares), SC70 (green diamonds), Ni04 (blue up triangles), Ni02 (purple down triangles), and NSC45 (black hexagons) at different $\hbar\omega$: (a)–(c) 5 meV, (d)–(f) 6.5 meV, and different temperature (a),(d) 5 K, (b),(e) 20–25 K, and (c),(f) 100 K. A flat fitted background has been subtracted from all data sets. The lines are based on the fits described in the text. The error bars represent the square root of the number of counts. The data for Ni02 and Ni04 are from Ref. [21].

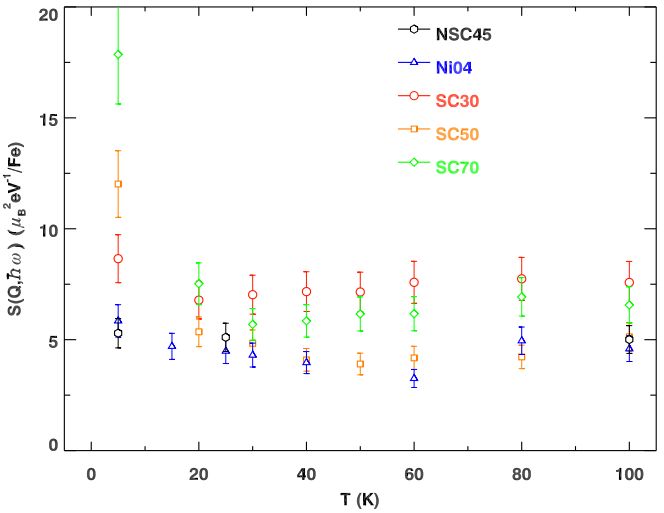



FIG. 4. (Color online) $\mathbf{Q}$-integrated (integrated only in one dimension, along the transverse direction) magnetic scattering intensity at $\hbar\omega = 6.5$ meV, obtained based on the fit described in the text, vs temperature for different samples: SC30 (red circles), SC50 (orange squares), SC70 (green diamonds), Ni04 (blue up triangles), and NSC45 (black hexagons).

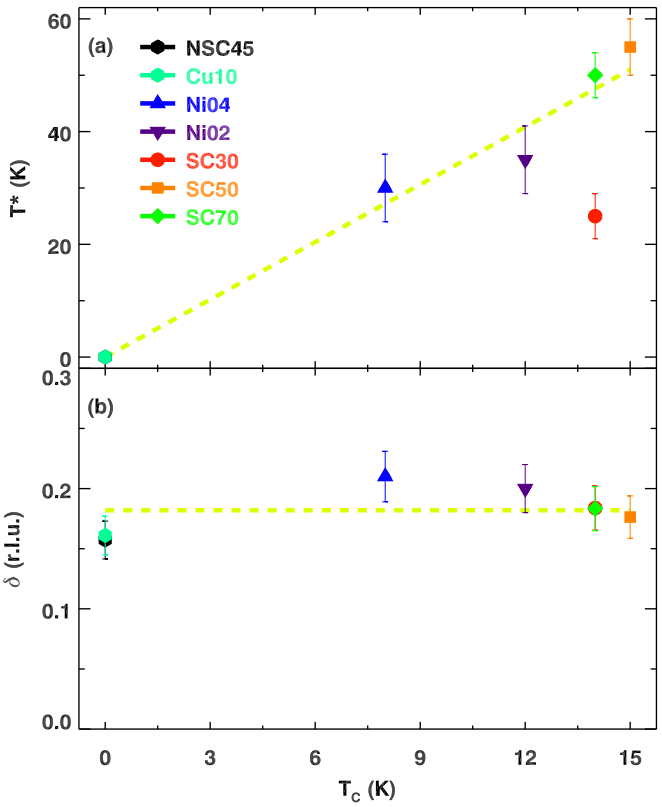



FIG. 5. (Color online) Summary of the fitting parameters of all samples. (a) The crossover temperature $T^*$ vs $T_c$ and (b) the incommensurability $\delta$ at 100 K vs $T_c$. SC30 (red circles), SC50 (orange squares), SC70 (green diamonds), Ni04 (blue up triangles), Ni02 (purple down triangles), Cu10 (teal hexagon), and NSC45 (black hexagons). The dashed lines are guides to the eye.

a coincidence cannot be resolved from these measurements, as we need to consider the full two-dimensional intensity map. To properly evaluate and interpret the thermal evolution of the magnetic correlations, we will need to map them throughout the (hk0) zone, an effort that we have just begun.

Plotting the crossover temperature $T^*$ versus $T_c$ in Fig. 5(a), we find a linear correlation between these quantities. The only exception is the SC30 sample, which is likely due to the complication in determining $T^*$ in this mixed-phase sample. The incommensurability $\delta$ at 100 K is plotted in Fig. 5(b). It is essentially independent of the superconducting properties.

## IV. SUMMARY

Overall, our results clearly suggest that the low-energy magnetic excitations in the "11" system are strongly correlated with the SC properties. When superconductivity is destroyed with either heating or chemical doping, the magnetic excitations move away from $\mathbf{Q}_{\mathrm{AF}}$, becoming incommensurate. In the normal state, the spectral weight (based on our absolute intensity measurements) and incommensurability measured at 100 K are insensitive to the low-temperature properties, which suggests that the incommensurate phases induced by heating or chemical doping are qualitatively similar as far as the low-energy spin dynamics is concerned. On the other hand, the magnetic excitations from the superconducting phase are distinct, occurring at an entirely different location in reciprocal space than those in the nonsuperconducting phases. This is quite intriguing, if one considers the similarities in the electronic structures across a range of "11" compounds. ARPES measurements on various "11" compounds, both superconducting and nonsuperconducting, with different Se concentrations or excess Fe [37–41], show that the band structure near the Fermi surface is qualitatively similar across a large doping range. The shape of the Fermi surface is relatively invariant with Se concentration, with hole pockets near the Γ point and electron pockets near the $M$ point [37–40]. No significant change in the shape of the Fermi surface or band structure has been reported in the temperature range of our measurements for samples without static magnetic order. The change of low-energy magnetic excitations across different samples or different phases in the same sample apparently is not compatible with the lack of change in the Fermi surface nesting conditions. Our results therefore provide yet another piece of evidence that the magnetic excitations in the "11" compounds cannot be simply explained by Fermi surface topology, and contributions from both localized and itinerant electrons have to be considered as suggested by previous experimental and theoretical work [35,42–45].

## ACKNOWLEDGMENTS

The work at Brookhaven National Laboratory and Lawrence Berkeley National Laboratory was supported by the Office of Basic Energy Sciences (BES), Division of Materials Science and Engineering, U.S. Department of Energy (DOE), under Contract Nos. DE-AC02-98CH10886 and DE-AC02-05CH1123, respectively. Research at Oak Ridge National Laboratory's High Flux Isotope Reactor was sponsored by the Division of Scientific User Facilities, BES, DOE.

[1] I. I. Mazin, Nature (London) **464**, 183 (2010).
[2] J. Paglione and R. L. Greene, Nat. Phys. **6**, 645 (2010).
[3] J. M. Tranquada, G. Xu, and I. A. Zaliznyak, J. Magn. Magn. Mater. **350**, 148 (2014).
[4] J. M. Tranquada, H. Woo, T. G. Perring, H. Goka, G. D. Gu, G. Xu, M. Fujita, and K. Yamada, Nature (London) **429**, 534 (2004).
[5] G. Xu, G. D. Gu, M. Hucker, B. Fauque, T. G. Perring, L. P. Regnault, and J. M. Tranquada, Nat. Phys. **5**, 642 (2009).
[6] J. Rossat-Mignod, L. P. Regnault, C. Vettier, P. Bourges, P. Burlet, J. Bossy, J. Y. Henry, and G. Lapertot, Physica C **185–189**, 86 (1991).
[7] P. Bourges, L. P. Regnault, Y. Sidis, and C. Vettier, Phys. Rev. B **53**, 876 (1996).
[8] P. Dai, H. A. Mook, G. Aeppli, S. M. Hayden, and F. Dogan, Nature (London) **406**, 965 (2000).
[9] H. F. Fong, P. Bourges, Y. Sidis, L. P. Regnault, A. Ivanov, G. D. Gu, N. Koshizuka, and B. Keimer, Nature (London) **398**, 588 (1999).

[10] S. M. Hayden, H. A. Mook, P. Dai, T. G. Perring, and F. Dogan, Nature (London) **429**, 531 (2004).
[11] B. Vignolle, S. M. Hayden, D. F. McMorrow, H. M. Ronnow, B. Lake, C. D. Frost, and T. G. Perring, Nat. Phys. **3**, 163 (2007).
[12] V. Hinkov, P. Bourges, S. Pailhes, Y. Sidis, A. Ivanov, C. D. Frost, T. G. Perring, C. T. Lin, D. P. Chen, and B. Keimer, Nat. Phys. **3**, 780 (2007).
[13] M. D. Lumsden and A. D. Christianson, J. Phys.: Condens. Matter **22**, 203203 (2010).
[14] A. D. Christianson, E. A. Goremychkin, R. Osborn, S. Rosenkranz, M. D. Lumsden, C. D. Malliakas, I. S. Todorov, H. Claus, D. Y. Chung, M. G. Kanatzidis, R. I. Bewley, and T. Guidi, Nature (London) **456**, 930 (2008).
[15] A. D. Christianson, M. D. Lumsden, K. Marty, C. H. Wang, S. Calder, D. L. Abernathy, M. B. Stone, H. A. Mook, M. A. McGuire, A. S. Sefat, B. C. Sales, D. Mandrus, and E. A. Goremychkin, Phys. Rev. B **87**, 224410 (2013).
[16] M. D. Lumsden, A. D. Christianson, D. Parshall, M. B. Stone, S. E. Nagler, G. J. MacDougall, H. A. Mook, K. Lokshin, T. Egami, D. L. Abernathy, E. A. Goremychkin, R. Osborn, M. A. McGuire, A. S. Sefat, R. Jin, B. C. Sales, and D. Mandrus, Phys. Rev. Lett. **102**, 107005 (2009).
[17] S. Chi, A. Schneidewind, J. Zhao, L. W. Harriger, L. Li, Y. Luo, G. Cao, Z. A. Xu, M. Loewenhaupt, J. Hu, and P. Dai, Phys. Rev. Lett. **102**, 107006 (2009).
[18] D. S. Inosov, J. T. Park, P. Bourges, D. L. Sun, Y. Sidis, A. Schneidewind, K. Hradil, D. Haug, C. T. Lin, B. Keimer, and V. Hinkov, Nat. Phys. **6**, 178 (2010).
[19] Y. Qiu, W. Bao, Y. Zhao, C. Broholm, V. Stanev, Z. Tesanovic, Y. C. Gasparovic, S. Chang, J. Hu, B. Qian, M. Fang, and Z. Mao, Phys. Rev. Lett. **103**, 067008 (2009).
[20] J. Wen, G. Xu, Z. Xu, Z. W. Lin, Q. Li, Y. Chen, S. Chi, G. Gu, and J. M. Tranquada, Phys. Rev. B **81**, 100513(R) (2010).
[21] Z. Xu, J. Wen, Y. Zhao, M. Matsuda, W. Ku, X. Liu, G. Gu, D.-H. Lee, R. J. Birgeneau, J. M. Tranquada, and G. Xu, Phys. Rev. Lett. **109**, 227002 (2012).
[22] N. Tsyrulin, R. Viennois, E. Giannini, M. Boehm, M. Jimenez-Ruiz, A. A. Omrani, B. D. Piazza, and H. M. Rønnow, New J. Phys. **14**, 073025 (2012).
[23] M. D. Lumsden, A. D. Christianson, E. A. Goremychkin, S. E. Nagler, H. A. Mook, M. B. Stone, D. L. Abernathy, T. Guidi, G. J. MacDougall, C. de la Cruz, A. S. Sefat, M. A. McGuire, B. C. Sales, and D. Mandrus, Nat. Phys. **6**, 182 (2010).
[24] P. Babkevich, M. Bendele, A. T. Boothroyd, K. Conder, S. N. Gvasaliya, R. Khasanov, E. Pomjakushina, and B. Roessli, J. Phys.: Condens. Matter **22**, 142202 (2010).
[25] W. Jinsheng, X. Guangyong, G. Genda, J. M. Tranquada, and R. J. Birgeneau, Rep. Prog. Phys. **74**, 124503 (2011).
[26] G. Xu, Z. Xu, and J. M. Tranquada, Rev. Sci. Instrum. **84**, 083906 (2013).
[27] Z. Xu, J. Wen, G. Xu, Q. Jie, Z. Lin, Q. Li, S. Chi, D. K. Singh, G. Gu, and J. M. Tranquada, Phys. Rev. B **82**, 104525 (2010).
[28] W. Bao, Y. Qiu, Q. Huang, M. A. Green, P. Zajdel, M. R. Fitzsimmons, M. Zhernenkov, S. Chang, M. Fang, B. Qian, E. K. Vehstedt, J. Yang, H. M. Pham, L. Spinu, and Z. Q. Mao, Phys. Rev. Lett. **102**, 247001 (2009).
[29] S. Li, Y. Chen, S. Chang, J. W. Lynn, L. Li, Y. Luo, G. Cao, Z. Xu, and P. Dai, Phys. Rev. B **79**, 174527 (2009).
[30] E. E. Rodriguez, C. Stock, P. Zajdel, K. L. Krycka, C. F. Majkrzak, P. Zavalij, and M. A. Green, Phys. Rev. B **84**, 064403 (2011).
[31] E. E. Rodriguez, D. A. Sokolov, C. Stock, M. A. Green, O. Sobolev, J. A. Rodriguez-Rivera, H. Cao, and A. Daoud-Aladine, Phys. Rev. B **88**, 165110 (2013).
[32] D. Parshall, G. Chen, L. Pintschovius, D. Lamago, T. Wolf, L. Radzihovsky, and D. Reznik, Phys. Rev. B **85**, 140515 (2012).
[33] I. A. Zaliznyak, Z. Xu, J. M. Tranquada, G. Gu, A. M. Tsvelik, and M. B. Stone, Phys. Rev. Lett. **107**, 216403 (2011).
[34] X. He, G. Li, J. Zhang, A. B. Karki, R. Jin, B. C. Sales, A. S. Sefat, M. A. McGuire, D. Mandrus, and E. W. Plummer, Phys. Rev. B **83**, 220502 (2011).
[35] Z. Xu, J. Wen, G. Xu, S. Chi, W. Ku, G. Gu, and J. M. Tranquada, Phys. Rev. B **84**, 052506 (2011).
[36] C. Stock, E. E. Rodriguez, and M. A. Green, Phys. Rev. B **85**, 094507 (2012).
[37] A. Tamai, A. Y. Ganin, E. Rozbicki, J. Bacsa, W. Meevasana, P. D. C. King, M. Caffio, R. Schaub, S. Margadonna, K. Prassides, M. J. Rosseinsky, and F. Baumberger, Phys. Rev. Lett. **104**, 097002 (2010).
[38] Y. Xia, D. Qian, L. Wray, D. Hsieh, G. F. Chen, J. L. Luo, N. L. Wang, and M. Z. Hasan, Phys. Rev. Lett. **103**, 037002 (2009).
[39] F. Chen, B. Zhou, Y. Zhang, J. Wei, H.-W. Ou, J.-F. Zhao, C. He, Q.-Q. Ge, M. Arita, K. Shimada, H. Namatame, M. Taniguchi, Z.-Y. Lu, J. Hu, X.-Y. Cui, and D. L. Feng, Phys. Rev. B **81**, 014526 (2010).
[40] E. Ieki, K. Nakayama, Y. Miyata, T. Sato, H. Miao, N. Xu, X.-P. Wang, P. Zhang, T. Qian, P. Richard, Z.-J. Xu, J. S. Wen, G. D. Gu, H. Q. Luo, H.-H. Wen, H. Ding, and T. Takahashi, Phy. Rev. B **89**, 140506(R) (2014).
[41] H. Yang (private communication).
[42] W.-G. Yin, C.-C. Lee, and W. Ku, Phys. Rev. Lett. **105**, 107004 (2010).
[43] S.-P. Kou, T. Li, and Z.-Y. Weng, Europhys. Lett. **88**, 17010 (2009).
[44] M. Wang, C. Zhang, X. Lu, G. Tan, H. Luo, Y. Song, M. Wang, X. Zhang, E. A. Goremychkin, T. G. Perring, T. A. Maier, Z. Yin, K. Haule, G. Kotliar, and P. Dai, Nat. Commun. **4**, 2874 (2013).
[45] P. Dai, J. Hu, and E. Dagotto, Nat. Phys. **8**, 709 (2012).